International Journal of Nanomedicine

Dovepress

open access to scientific and medical research

Open Access Full Text Article

ORIGINAL RESEARCH

Macrophage-Targeted Berberine-Loaded β-Glucan Nanoparticles Enhance the Treatment of Ulcerative Colitis

Yuying Xu[1,*], Jintao Huang[2,*], Yapei Fan[1], Haiyue Long[1], Minting Liang[1], Qunjie Chen[1], Zhiping Wang[2], Chaoxi Wu[1], Yifei Wang[1]

[1]Department of Cell Biology, College of Life Science and Technology, Jinan University, Guangzhou, People's Republic of China; [2]Guangdong Provincial Engineering Center of Topical Precise Drug Delivery System, School of Pharmacy, Guangdong Pharmaceutical University, Guangzhou, People's Republic of China

*These authors contributed equally to this work

Correspondence: Chaoxi Wu; Yifei Wang, Email chaoxiw@gmail.com; twang-yf@163.com

Aim: This study focuses on constructing of an anti-inflammatory drug delivery system by encapsulation of berberine in the β-glucan nanoparticles and evaluates its effect on treating ulcerative colitis.

Methods: β-Glucan and the anti-inflammatory drug berberine (BER) are self-assembled into nanoparticles to construct a drug delivery system (GLC/BER). The interaction between the drug and the carrier was characterized by circular dichroism, ultraviolet-visible spectroscopy, and dynamic light scattering. The anti-inflammatory effect of the GLC/BER was evaluated through a lipopolysaccharide (LPS)-induced RAW264.7 macrophage inflammation model and a sodium sulfate (DSS)-induced C57BL/6 mouse ulcerative colitis model.

Results: The GLC/BER nanoparticles have a particle size of 80–120 nm and a high encapsulation efficiency of 37.8±4.21%. In the LPS-induced RAW264.7 macrophage inflammation model, GLC/BER significantly promoted the uptake of BER by RAW264.7 cells. RT-PCR and ELISA assay showed that it could significantly inhibit the inflammatory factors including IL-1β, IL-6 and COX-2. Furthermore, GLC/BER shows inhibiting effect on the secretion of pro-inflammatory factors such as IL-1β and IL-6, down-regulating the production of nitrite oxide; in animal studies, GLC/BER was found to exert a relieving effect on mice colitis.

Conclusion: The study found that GLC/BER has an anti-inflammatory effect in vitro and in vivo, and the GLC carrier improves the potency and bioavailability of BER, providing a new type of nanomedicine for the treatment of colitis.

Keywords: β-glucan, chiral, drug carrier, immunoregulation, anti-inflammation

Introduction

Inflammatory bowel disease (IBD) is a non-specific chronic intestinal inflammatory disease that mainly includes ulcerative colitis (UC) and Crohn's disease (CD).[1,2] IBD is a common disease in Europe and America, and the incidence of IBD increases year by year in China.[3] Inflammatory bowel disease may invade any part of the gastrointestinal tract and induce extra-intestinal manifestations. Patients with IBD often present with symptoms such as inflammation, diarrhea, abdominal pain, bloody stool, and weight loss.[4,5] Treatment of IBD generally commonly starts with drug therapy, such as corticosteroids,[6] amino salicylates,[7] antibiotics,[8] supportive drugs[9] and immunosuppressive drugs.[10] Therapeutic drugs take effect quickly, but often suffer from various side effects. Natural compounds extracted from vegetable or fruit can not only suppress intestinal inflammation but also improve intestinal epithelial barrier function and regulate intestinal flora.[11,12] To deliver natural compounds to gut without damage by gastric acid, nano-delivery systems may be a promising solution. Compared with synthetic nanoparticles, biopolymer nanoparticles have advantages of high

Received: 11 July 2022
Accepted: 4 November 2022
Published: 14 November 2022

biocompatibility and biodegradability. Nanoparticles based on gelatin,[13] cellulose,[14] and chitosan[15] have been used to deliver anti-inflammatory compounds to colonic epithelium with improved therapeutic effects.

β-Glucan is a natural polysaccharide with immune-modulating activities which can be developed as adjuvants in anti-inflammatory,[16] anti-cancer,[17] anti-bacterial[18] and anti-viral therapies.[19] β-Glucan can be found in biological tissues such as fungi cell wall or bacterial secreta where the glucan chains are packed in highly stable triple helical conformation. β-Glucan can take up to 40% of the dry mass of yeast cell wall.[20,21] Previous studies has used yeast cell wall as a delivery vehicle to deliver a wide range of drugs to immune cells.[22–24] However, the preparation process of cell wall-based delivery vehicle is complex and difficult to control. The size of cell wall is typically ~5 μm, which must be sharply reduced if a nanoparticle delivery vehicle is intended. β-Glucan is packed in crystalline fibrillar form in cell wall, which cannot be easily disassembled and dissolved in cold or hot water.[25] A number of solvent systems can be used to dissolve β-glucan such as formic acid, diluted NaOH/water solution and organic solvent like Li/DMAc or DMSO.[26–29] β-Glucan can be dissolved in alkaline solution containing 0.1–0.2 M NaOH. When water was added in β-glucan/NaOH solution, β-glucan chains can renature into triple helix and further pack into nanoparticles. The solvent-driven self-assembly process of β-glucan in solution can be exploited to load drugs and construct β-glucan-based nanoparticle drug delivery systems.[30,31] However, up to now, there have been no reports of berberine-loaded β-glucan nanoparticles as anti-inflammatory drug delivery system.

In this study, we prepared an anti-inflammatory nano-delivery system based on berberine (BER) and yeast β-glucan (GLC) through solvent-driven self-assembly. The main assumption is that the helical structure of GLC can carry and deliver the drug BER specifically to macrophage cells and relieve DDS-induced colitis (Figure 1). The encapsulation of BER by GLC is studied by UV-Vis and circular dichroism spectroscopy. The drug release profile is studied at different pH conditions simulating pathological and healthy intestinal microenvironment. The anti-inflammatory effects of GLC/BER were first evaluated by its ability to inhibit the production of inflammatory-related mRNA, NO and cytokines in a RAW 264.7 cell model. Later, the GLC/BER was administered orally in a DDS-induced mice colitis model to study its effects on the treatment of ulcerative colitis.

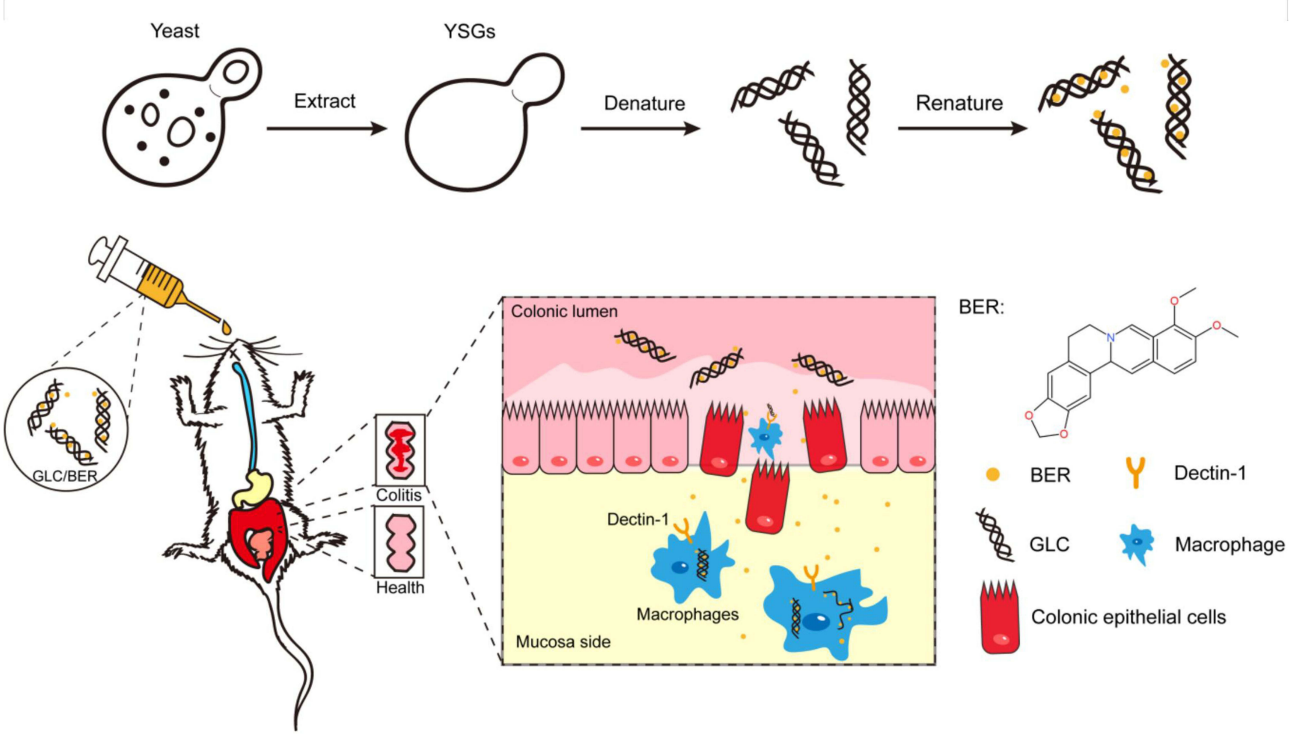

Figure 1 The preparation of GLC/BER and the proposed therapeutic effect on colitis.

Experimental Section

Materials

Yeast cell wall particles (Baker's yeast) were purchased from Tiantian Bioengineering & Technology Co., Ltd (China) (purity: 99%). Berberine (BER) was purchased from Yuanye Bio-Technology (Shanghai, China). Dulbecco's Modified Eagle Medium (DMEM, glutamine, high glucose), penicillin, streptomycin and fetal bovine serum (FBS) were purchased from HyClone (USA). Dialysis tube (MW cutoff, 1.4 kDa) was purchased from Spectrum Labs (Seoul, Korea). Other reagents used in this work were purchased from Shanghai Aladdin Chemicals unless otherwise specified.

Preparation of GLC and GLC/BER

GLC and GLC/BER were prepared by pH-induced self-assembly. For the GLC, powder of β-glucan was suspended in deionized water (1 mg/mL, 9 mL). To the suspension, NaOH solution was added to adjust the pH to 13.0. For the GLC/BER, 1.0 mL of BER water solution (BER: 1.0 mg/mL) was added and the resulting mixture was stirred for 5 min. Next, HCl solution was added into the mixture solution to adjust the pH to 7.4. Free BER was removed by dialysis in water for 2 d.

Characteristics

Drug loading capacity. The drug loading efficiency (DLE) was defined as the weight percentage of BER in the GLC, and drug encapsulation efficiency (DEE) was defined as the weight percentage of loaded-BER in the GLC and the given BER. Firstly, BER solutions of various concentrations were prepared, and the absorbance at 481 nm was measured to generate a calibration curve for the DLE and DEE calculations from various GLC. Secondly, in order to determine the DLE and DEE, 2.0 mg of lyophilized complex was dispersed in 1 mL of deionized water at room temperature, followed by dilution with 9 mL of DMSO to completely expose the encapsulated BER. The obtained solution was examined by UV–vis spectroscopy at a wavelength of 345 nm. DLE (%) and DEE (%) were calculated according to the following equations:

$$\text{DLE } (\%) = \frac{\text{the weight of drug loaded into nanogel}}{\text{the total weight of drug carrier}} \times 100\%$$

$$\text{DLE } (\%) = \frac{\text{the weight of drug loaded into nanogel}}{\text{the total weight of drug carrier}} \times 100\%$$

Ultraviolet and visible spectrum (UV−vis). Absorption spectra from the GLC, GLC/BER solution were taken with a double-beam UV−vis spectrometer (Shimadzu UV-2101PC) in a 0.1 mm/0.2 mm demountable quartz cell (Hellmar GmbH, Germany) with the range of 200−400 nm.

Circular Dichroism spectra (CD). The CD spectra were recorded on a Chirascan CD spectrophotometer (Applied Photophysics, UK). CD spectra were determined over the range of 300−400 nm using a quartz cell with 0.1 mm path length. Scans were taken at a rate of 30 nm/min with a sampling interval of 1.0 nm and response time of 1 s at room temperature.

Diameter and size distribution. The diameter and size distribution of the obtained GLC, GLC/BER were evaluated by dynamic light scattering (DLS, Malvern Nano-ZS, UK) at sample concentration 1.0 mg/mL.

Transmission electron microscopy (TEM). TEM micrographs of the nanoparticles esters were taken with a Hitachi 7650 transmission electron microscope with an acceleration voltage of 80 kV. The particles were stained with a 2% aqueous solution of phosphotungistic acid and were deposited on a carbon-coated grid without any treatments.

Drug release in vitro. The BER release was assessed in simulated gastric fluid (pH 1.2, 0.04 m HCl, 2 h), intestinal fluid (pH 6.8, 0.1 m PBS buffer, 4 h) and colon fluid (normal: pH 7.4, 0.1 m PBS buffer; IBD: pH 3.5, 0.1 m PBS buffer adjusted by HCl, 42 h) to simulate normal and colitis gastrointestinal tract (GI) with a dialysis method. In detail, 5 mg GLC/BER dispersed in 1 mL 0.9% NaCl solution was dialyzed using a dialysis tube (M_wCO 8000−12,000) against 80 mL of simulating buffer under gentle shaking (70 rpm) at the constant temperature of 37°C; 1 mL of simulating medium containing the released BER was collected for UV measurement at desired time points, followed by replenishing rapidly equal volume of fresh medium. The concentration of the released drug in the collected medium was measured

using a UV–vis spectrophotometer at 345 nm, and the accumulated drug release was calculated. All the drug loading and release experiments were performed in triplicate to determine means and SD.

Cell Experiments

Cell culture. Monocyte-like macrophage RAW264.7 cell and epithelial cell Caco-2 were purchased from Nanjing Cobioer Biosciences Co., LTD. Cells were cultured in Dulbecco's Modified Eagle's Medium (DMEM) supplemented with 10% fetal bovine serum, 100 IU/mL penicillin, and 100 μg/mL streptomycin at 37°C in a humidified atmosphere with 5% CO_2.

Cellular uptake. The cellular uptake of GLC/BER and free BER were examined by fluorescence microscopy. Briefly, RAW264.7 (5×10^5 cells per well) and Caco-2 (2×10^5 cells per well) at logarithm phase were seeded in 24 well cell culture plates, respectively. After incubated for 24 h, GLC/BER or free BER dissolved in PBS at 5 mg/L was added to replace the media in each well. After further incubated for 1 h, and 4 h, the media were removed and these wells were rinsed with PBS (pH = 7.4) and then were observed using Nikon microscope (TE2000-U, Nikon, Japan).

Reverse transcription-PCR (RT-PCR). Total RNA was extracted from RAW264.7 cells using Trizol reagent (Invitrogen Corp., USA), according to the manufacturer's instructions. cDNAs were synthesized from 1 μg of total RNA from each sample using a high-capacity cDNA reverse transcription kit (Applied Biosystems, USA) and were amplified with mouse-specific primers for COX-2, IL-1β, IL-6.

Western blotting analysis (WB). Total proteins from RAW264.7 cells were extracted and analyzed by Western blotting according to the reported method.

Cytokine assay. NO concentration in the medium supernatant of RAW264.7 cells was determined by the Griess reaction. IL-1β and IL-6 cytokines were assessed using ELISA kits according to the manufacturer's instructions (Dakewe Biotech Corporation).

Animals and Experimental Protocols

Eight-week-old female C57BL/6 mice weighing 18–20 g were purchased from the Guangdong Medical Laboratory Animal Center. All animal procedures were approved by the Committee on Animals of the Jinan University. All animal procedures were performed in accordance with the guidelines of the Committee on Animals of the Jinan University (No. SQ2021-0241).

Mice were housed under controlled room temperature (22 ± 2 °C) and humidity (55 ± 5%) on a 12 h light–dark cycle with free access to water and diets, and were randomly divided into 5 groups (the control group; 3% DSS group; 3% DSS + 60 mg/kg/day GLC group; 3% DSS + 2.2mg/kg/day BER group, 3% DSS + 60 mg/kg/day GLC/BER group, 5 mice/group). The mice in the control group were supplied with distilled water, whereas all other experimental groups were given 3% DSS from day 1 to day 5 and supplied with distilled water from day 6 to day 10. Besides, the mice in the GLC, BER, and GLC/BER-treated groups were administered by gavage from day 1 to day 9 and the mice in CTRL and DSS group were administered with equal volume of saline as comparison, respectively.

Evaluation of disease activity index (DAI). The DAI was established by scoring the changes in body weight loss, diarrheal condition and fecal bleeding. The DAI is the sum of the score of these three parameters. Each score was determined according to the reported method. At the end of the experiment, all mice were sacrificed; colons were dissected from each mouse, and the lengths between the ileo-cecal junction and anal verge were measured.

Histological Score. The harvested colons of mice were gently washed with ice-cold PBS, fixed in 4% paraformaldehyde overnight and embedded in paraffin. After slicing, hematoxylin and eosin (H&E) staining was performed. The histological scoring system is determined according to the reported method.

Result and Discussion

Characterizations of GLC/BER

Photos of GLC, BER and GLC/BER in solution are shown in Figure 2A. It can be seen that BER has poor solubility in water and large insoluble aggregates can be seen inside of the vial. In contrast, the suspension of GLC/BER was highly

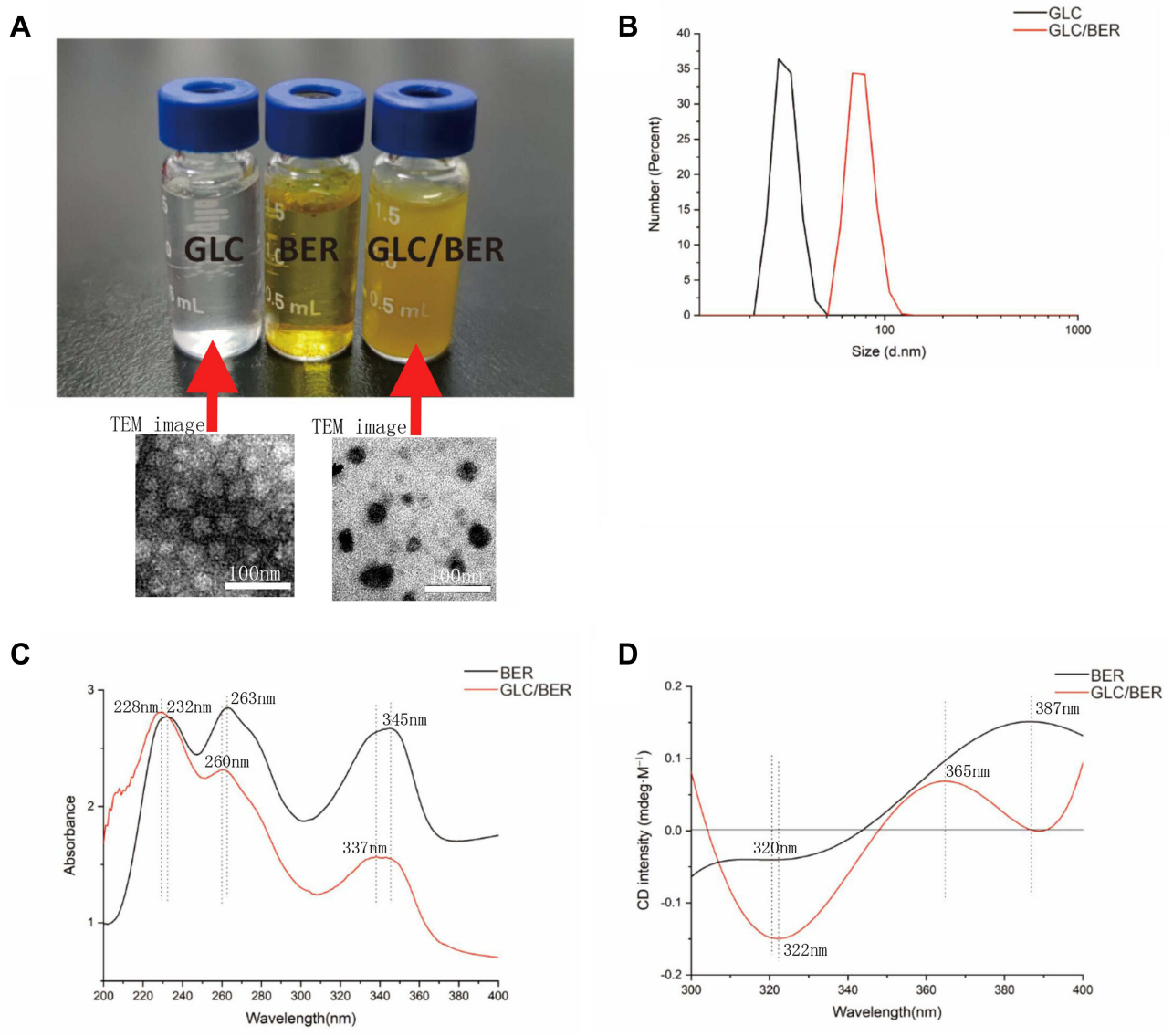

Figure 2 Characterizations of GLC and GLC/BER. Photographs of GLC, BER and GLC/BER in solution, Inset: TEM images of the nanoparticles (**A**); DLS results and particle size distribution of GLC and GLC/BER (**B**); UV spectrum analysis of BER and GLC/BER (**C**); CD spectra of BER and GLC/BER (**D**).

homogeneous with no visible precipitation, suggesting that the dispersion of BER can be improved by GLC. In addition, GLC/BER remained stable after 2 months with no visible aggregation or precipitation, indicating a high extent of stability. Figure 2B shows the nanoparticle size distribution of GLC and GLC/BER using dynamic light scattering. As shown in the figure, the size of individual GLC is distributed between 30 nm and 60 nm with an average particle size of 32 nm, while the size of GLC/BER is distributed between 60 nm and 120 nm with an average particle size of 72 nm. TEM images show that the GLC and GLC/BER nanoparticles have a spherical morphology and the particle size was increased after the drug loading process. The increase in particle size can be interpreted as the encapsulation of BER in GLC nanoparticles.

UV-Vis spectroscopy was used to study the interaction between GLC and BER. As is shown in Figure 2C, BER shows 3 distinctive peaks at 232, 263 and 345 nm, respectively. After complexed with GLC, the λ_{max} of the peaks red-shifted to 228, 260 and 337 nm, respectively, and the latter two peaks show a significant decline of intensity. This red-shift is commonly seen when hydrophobic molecules were encapsulated inside of the helical structure of β-glucan, indicating that BER may form non-covalent complex with GLC.

Circular dichroism spectroscopy was used to study the interaction between GLC and BER. As β-glucan is a helical polysaccharide with distinctive chirality, it can affect the CD signals of hosted molecules when special interaction occurred. As is shown in Figure 2D, the CD spectra of BER alone shows a negative shoulder peak at around 322 nm and a positive peak at 387 nm. After complex of BER with GLC, the CD spectra change significantly. The shower peak at 322 nm transformed into a sharp peak with increased intensity, and the positive peak shifted from 387 nm to 365 nm (22 nm of red-shift). As β-glucan has no CD signals due to the lack of chromophores on the backbone, the change of CD signals can be directly attributed to the encapsulation of BER in the helical structures of β-glucan. Taken together, the results demonstrated that the hydrophobic drug BER can be loaded in the helical structures of GLC in the form of homogeneously dispersed nanoparticles.

Entrapment Efficiency and Release Rate of GLC/BER

As shown in Table 1, β-glucan was used as the drug carrier to carry BER, and the content of BER in GLC/BER was determined to be 3.78%, with encapsulation efficiency of 28.4%. To explore the bioavailability of BER and further investigate the drug release characteristics of GLC/BER in a simulated intestinal environment. Simulating pH environment of normal colon (pH = 7.4) and colitis lesion colon (pH = 3.5), to explore the cumulative drug release rate of GLC/BER in gastrointestinal tract environment with different pH values. The results are shown in Figure 3. The cumulative release in the acidic environment of simulated colitis lesion was increased compared with normal condition, and the cumulative release rate of GLC/BER in the colon region 24 h reached about 20.57%. The above results indicated that GLC/BER could improve the bioavailability of BER and facilitate targeted delivery of BER to immune cells located in the colon area, thus exerting a good anti-inflammatory effect.

Macrophage Targeting Effects of GLC/BER

It is well established that β-glucan can be recognized by the pattern recognition receptors on host immune cells and can be used as a natural targeting motif for macrophages. Macrophages are one of the major immune cells that penetrate into the inflammation site and generate inflammatory factors. In order to evaluate the targeting ability of GLC/BER for macrophages, a series of cellular uptake assays were performed using RAW264.7 cells with a control group of Caco-2 cells (an epithelial cell line). RAW264.7 and Caco-2 cells were incubated with GLC/BER suspension, and imaged by a fluorescence microscopy. As is shown in Figure 4, there is no difference in the absorption of BER and GLC/BER by the RAW 264.7 cells at 1h. However, a robust green fluorescence can be observed in macrophage cells after treatment with the GLC/BER at 4h, while BER alone is hardly internalized under the same condition. The results indicate that GLC can promote the uptake of BER by macrophages, therefore increasing the bioavailability of BER. In contrast, GLC/BER was hardly internalized by Caco-2 cells at a similar condition, indicating that GLC/BER has no targeting effects for non-immune cells.

The in vitro Anti-Inflammatory Effects of GLC/BER

According to reports, COX-2, IL-1β, IL-6 and other inflammatory cytokines are related to the pathogenesis of many diseases, such as rheumatoid arthritis, Crohn's disease and encephalomyelitis. LPS is the active substance of gram-negative bacteria, which are well-known macrophage activators that can activate Toll-like receptor 4 (TLR4), inducing RAW264.7s macrophage cells to produce large amounts of NO and other inflammatory factors, such as IL-1β, IL-6, etc. Therefore, RAW264.7 inflammatory cell model stimulated by LPS was employed to study the anti-inflammatory activity of GLC/BER drug delivery by RT-qPCR experiments. As is shown in Figure 5A–C, GLC/BER exhibits strong inhibition effect on the production of inflammatory-related mRNA including COX-2, IL-1β, IL-6 in RAW264.7 cells; down-regulate

Table 1 Drug Loading Efficiency and Drug Encapsulation Efficiency of GLC/BER

Drug Carrier	Drug Loading Efficiency	Drug Encapsulation Efficiency
GLC/BER	3.53%	35.3%

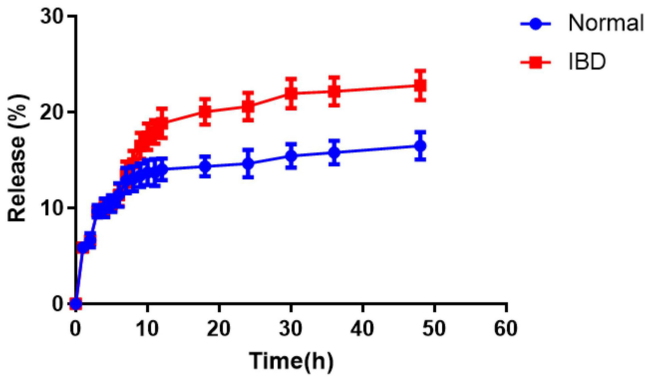

Figure 3 Cumulative release statistics of GLC/BER in vitro under different gastrointestinal conditions (48h).

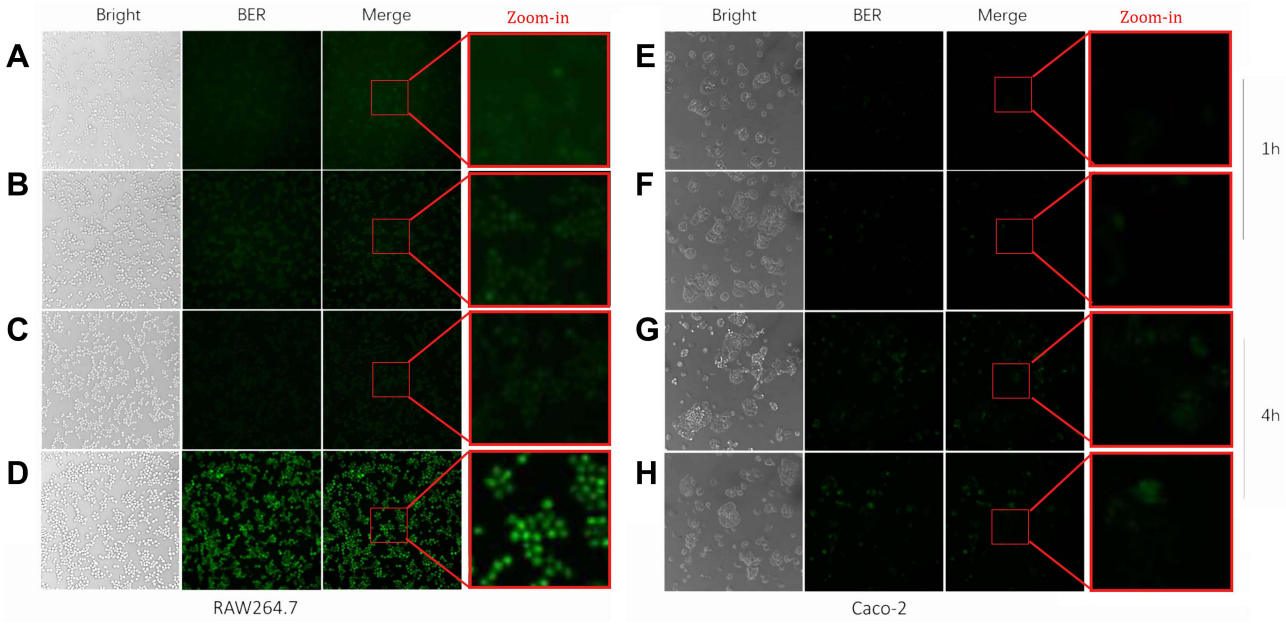

Figure 4 The uptake of BER (**A, C, E** and **G**) and GLC/BER (**B, D, F** and **H**) in RAW264.7/Caco-2 cells was determined after incubation for 1h and 4h.

s the secretion of NO in a Griess assay; and decrease the secretion of inflammation-associated factors of IL-1β and IL-6 measured by ELISA experiment. The anti-inflammatory effects of GLC/BER is also higher than that of GLC and BER alone.

GLC/BER Alleviates DSS-Induced Colitis in Mice

The DSS-induced acute colitis model in mice is simple to establish and has similar characteristics to human ulcerative colitis. Therefore, it is widely used in the research of inflammatory bowel disease. Because GLC/BER can promote the effect of macrophages on drugs ingestion and significantly inhibit LPS-induced cell inflammation, the therapeutic effect of GLC/BER in acute colitis was further evaluated. The experimental protocol of this study is shown in Figure 6A. First, 3% DSS was used to create a model for 5 days, and the drug was administered on the first day of model building for a total of 9 days. Finally, the mice were killed on the 10th day and the samples were taken.

Weight change and colitis animal disease activity index are the criteria for evaluating colitis modeling and treatment effects. First, as shown in Figure 5B and C, the body weight of the mice in the normal group increased during the test, while the DSS model mice began to lose weight significantly on the sixth day of the experiment, and reached the lowest

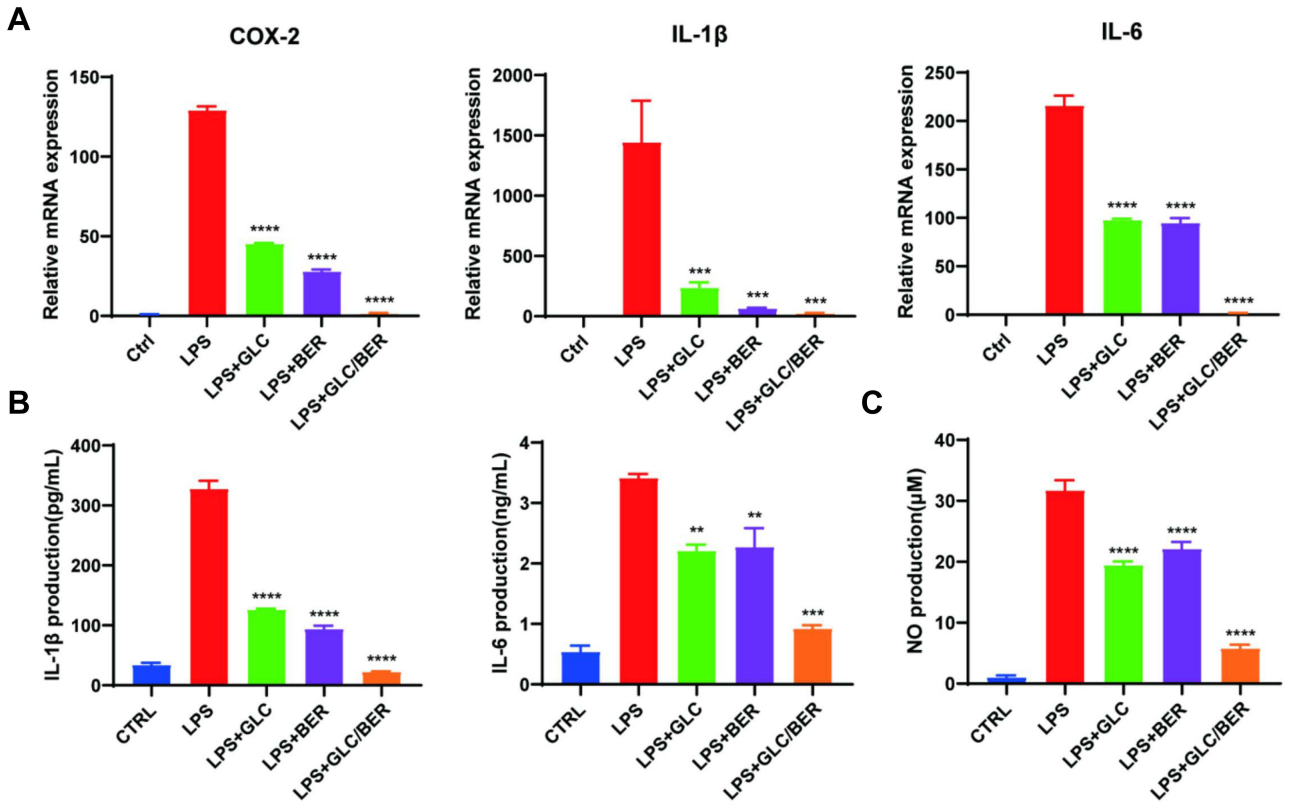

Figure 5 The effects of GLC, BER and GLC/BER on the mRNA expression of COX-2, IL-1β, IL-6 (**A**) and IL-1β, IL-6 (**B**) and NO (**C**) secretion of RAW264.7 macrophages induced by LPS after incubation for 12 hours. Each value represents the mean ±SEM of three separate experiments. Each group was compared with the cell blank control group. **p<0.01, ***p<0.001, ****p<0.0001.

value on the eighth day. In addition, DSS model mice developed drowsiness, loose stools, and bloody stools. Severe diarrhea began on the fifth day. Obvious weight loss and clinical symptoms showed that 3% DSS successfully induced colitis. Compared with the DSS group, mice in the GLC, BER, and GLC/BER groups also showed similar clinical symptoms after the sixth day. In addition, the weight loss of GLC group and BER group was similar to that of DSS group, indicating that β-glucan and berberine alone had no significant therapeutic effect on colitis, while the weight loss rate of GLC/BER group mice was the slowest, and maintained the minimum weight loss rate in all the administration groups, indicating that GLC/BER has a better therapeutic effect.

In view of the DSS successfully induced severe clinical symptoms in mice with colitis, the mice's drinking water was replaced with normal water from the sixth day to slightly alleviate the over-severe colitis in mice. After alleviation and continuous administration treatment, the mice in the GLC/BER administration group were the first to regain their vitality and stopped appearing blood in the stool at the same time, while the other administration groups were not much different from the model. The above results indicate that DSS can successfully induce colitis in mice, while the GLC, and BER groups have no efficacy in treating colitis in mice. This can be attributed to the fact that the GLC/BER drug carrier group can effectively improve the bioavailability of BER, so as to treat colitis in mice and alleviate the rapid weight loss of mice.

In addition, the length of the colon and histopathological section are also important criteria for evaluating the severity of colitis. As shown in the Figure 6D and E, the average length of the colon of the control group is significantly longer than that of the DSS group, which is consistent with the data reported that DSS-induced colitis will cause the colon to shorten. Compared with the DSS group, it can be observed that the GLC/BER group has increased colon length, indicating that the GLC/BER group can partially alleviate DSS-induced colitis.

The histopathological section of the colon was further evaluated. As is shown in Figure 7, DSS caused severe mucosal damage, crypt loss, and necrosis. At the same time, extensive macrophage infiltration can be observed. Macrophages play

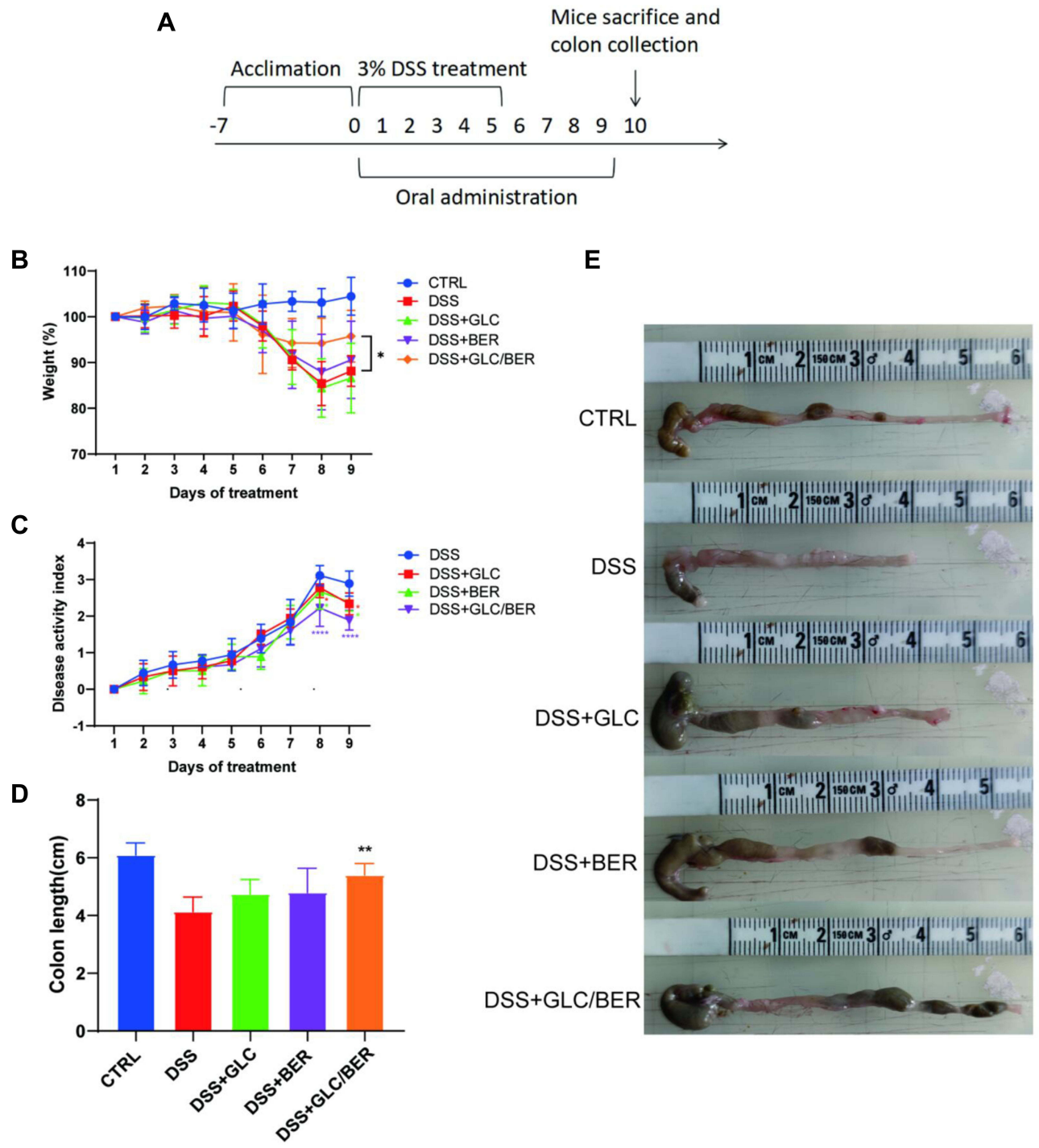

Figure 6 Effects of GLC/BER on alleviating the symptoms of DSS-induced colitis in mice. Experimental protocol of DSS -nduced colitis in mice (**A**); Body weight change (**B**); DAI score (**C**); Statistical analysis of colon length (**D**); Representative view of colon (**E**). Data were presented as mean standard deviation (n=6). Each group was compared with the DSS group, *P<0.05, **P<0.01, ****P<0.0001.

a key role in the pathophysiology of colitis, and their infiltration of the colon can aggravate inflammation. As is shown in the histopathological images, GLC/BER-treated group shows a relieved symptoms of macrophage infiltration and damage of colonic tissues. The possible reason is that GLC promotes cell internalization through related receptors on the cell surface of macrophages, thereby increasing the uptake and anti-inflammatory effect of BER.

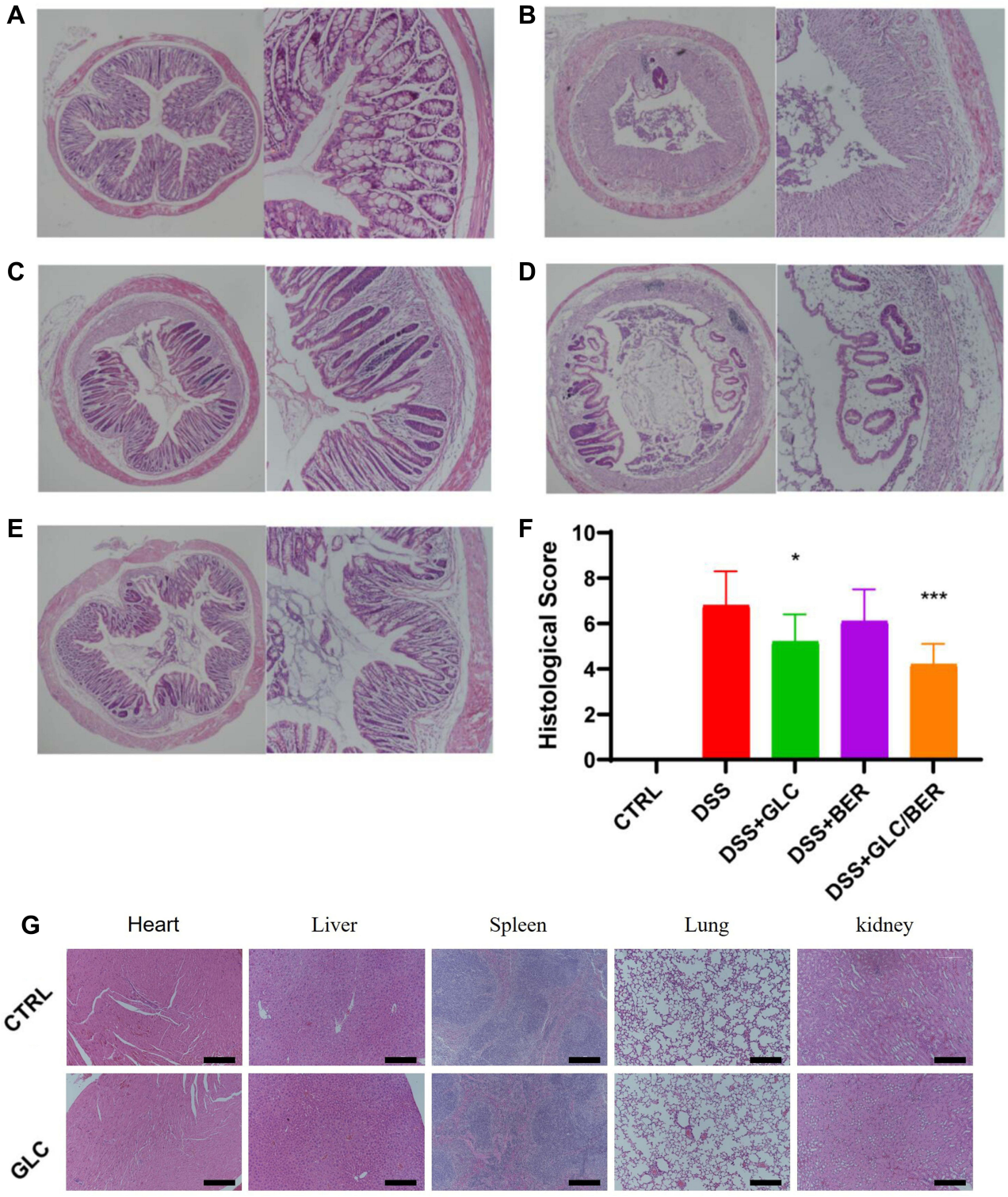

Figure 7 H&E staining of colonic sections at 100 and 200 magnification. CTRL (**A**); DSS (**B**); DSS+GLC (**C**); DSS+BER (**D**); DSS+GLC/BER (**E**); Colon histopathological injury score (**F**). Organ tissue sections of control and GLC groups (**G**), *P<0.05, ***P<0.001.

Conclusions

The yeast-derived β-glucan is used to construct a drug delivery vehicle, which effectively delivers the drug molecule berberine to the colon site and plays a significant role in the treatment of colon inflammation. The experimental results showed that β-glucan with triple helix structure can encapsulate BER at a high drug loading efficiency. GLC/BER can promote the uptake of berberine by macrophages, inhibit LPS-induced inflammation in RAW264.7 cell model, and alleviate the tissue damage caused by DDS-induced ulcerative colitis in a mice model. This work provides a new insight for the development of oral drug delivery systems for the treatment of colitis.

Acknowledgment

This project is supported by Guangdong Provincial Department of Education University Characteristic Innovation Project (2020KTSCX060), and Fundamental Research Funds for the Central Universities (21621006). Undergraduate Innovation and Entrepreneurship Training Program of Guangdong Pharmaceutical University (202210573062).Special Funds for Economic Development of Marine Economy of Guangdong Province, China (GDNRC [2022] 38).

Disclosure

The authors report no conflicts of interest in this work.

References

1. Li S, Wu B, Fu W, Reddivari L. The anti-inflammatory effects of dietary anthocyanins against ulcerative colitis. *Int J Mol Sci*. 2019;20(10):2588. doi:10.3390/ijms20102588
2. Hodson R. Inflammatory bowel disease. *Nature*. 2016;540(7634):S97. doi:10.1038/540S97a
3. Friedrich MJ. Inflammatory bowel disease goes global. *JAMA*. 2018;319(7):648.
4. Tsang L, Banerjee N, Tabibian JH. Bloody diarrhea and weight loss in a patient in remission from ulcerative colitis. *Gastroenterology*. 2019;157(5):1207–1209. doi:10.1053/j.gastro.2019.01.272
5. Bitzer ZT, Elias RJ, Vijay-Kumar M, Lambert JD. (-)-Epigallocatechin-3-gallate decreases colonic inflammation and permeability in a mouse model of colitis, but reduces macronutrient digestion and exacerbates weight loss. *Mol Nutr Food Res*. 2016;60(10):2267–2274. doi:10.1002/mnfr.201501042
6. Ben-Horin S, Har-Noy O, Katsanos KH, et al. Corticosteroids and mesalamine versus corticosteroids for acute severe ulcerative colitis: a randomized controlled trial. *Clin Gastroenterol Hepatol*. 2022. doi:10.1016/j.cgh.2022.02.055
7. He L, Wen S, Zhong Z, et al. The synergistic effects of 5-aminosalicylic acid and vorinostat in the treatment of ulcerative colitis. *Front Pharmacol*. 2021;12:625543. doi:10.3389/fphar.2021.625543
8. Miyoshi J, Miyoshi S, Delmont TO, et al. Early-life microbial restitution reduces colitis risk promoted by antibiotic-induced gut dysbiosis in interleukin 10(-/-) mice. *Gastroenterology*. 2021;161(3):940–952 e915. doi:10.1053/j.gastro.2021.05.054
9. Manzini R, Schwarzfischer M, Atrott K, et al. Combination of vedolizumab with tacrolimus is more efficient than vedolizumab alone in the treatment of experimental colitis. *Inflamm Bowel Dis*. 2021;27(12):1986–1998. doi:10.1093/ibd/izab063
10. Vedamurthy A, Xu L, Luther J, et al. Long-term outcomes of immunosuppression-naive steroid responders following hospitalization for ulcerative colitis. *Dig Dis Sci*. 2018;63(10):2740–2746. doi:10.1007/s10620-018-5176-3
11. Li S, Wang T, Wu B, et al. Anthocyanin-containing purple potatoes ameliorate DSS-induced colitis in mice. *J Nutr Biochem*. 2021;93:108616. doi:10.1016/j.jnutbio.2021.108616
12. Gowd V, Kanika JC, Jori C, et al. Resveratrol and resveratrol nano-delivery systems in the treatment of inflammatory bowel disease. *J Nutr Biochem*. 2022;109:109101. doi:10.1016/j.jnutbio.2022.109101
13. Ahmad A, Ansari MM, Mishra RK, et al. Enteric-coated gelatin nanoparticles mediated oral delivery of 5-aminosalicylic acid alleviates severity of DSS-induced ulcerative colitis. *Mater Sci Eng*. 2021;119:111582. doi:10.1016/j.msec.2020.111582
14. Ahmad A, Ansari MM, Kumar A, Bishnoi M, Raza SS, Khan R. Aminocellulose- grafted polycaprolactone-coated core–shell nanoparticles alleviate the severity of ulcerative colitis: a novel adjuvant therapeutic approach. *Biomaterial Sci*. 2021;9(17):5868–5883. doi:10.1039/D1BM00877C
15. Jin M, Li S, Wu Y, Li D, Han Y. Construction of chitosan/alginate nano-drug delivery system for improving dextran sodium sulfate-induced colitis in mice. *Nanomaterials*. 2021;11(8):1884. doi:10.3390/nano11081884
16. Šalamúnová P, Cupalová L, Majerská M, et al. Incorporating natural anti-inflammatory compounds into yeast glucan particles increases their bioactivity in vitro. *Int J Biol Macromol*. 2021;169:443–451. doi:10.1016/j.ijbiomac.2020.12.107
17. Wu LJ, Zhao J, Zhang XN, Liu S, Zhao CY. Antitumor effect of soluble l3-glucan as an immune stimulant. *Int J Biol Macromol*. 2021;179:116–124. doi:10.1016/j.ijbiomac.2021.02.207
18. Song J, Chen H, Wei Y, Liu J. Synthesis of carboxymethylated beta-glucan from naked barley bran and its antibacterial activity and mechanism against Staphylococcus aureus. *Carbohydr Polym*. 2020;242:116418. doi:10.1016/j.carbpol.2020.116418
19. Wang Y, Harding SV, Thandapilly SJ, Tosh SM, Jones PJH, Ames NP. Barley beta-glucan reduces blood cholesterol levels via interrupting bile acid metabolism. *Br J Nutr*. 2017;118(10):822–829. doi:10.1017/S0007114517002835
20. Klis FM, Boorsma A, De Groot PWJ. Cell wall construction in Saccharomyces cerevisiae. *Yeast*. 2006;23(3):185–202. doi:10.1002/yea.1349

21. Takeo K, Mine H, Nishimura K, Miyaji M. The existence of a dispensable fibrillar layer on the wall surface of mycelial but not yeast cells of Aureobasidium pullulans. *FEMS Microbiol Lett*. 1993;111(2–3):153–158. doi:10.1111/j.1574-6968.1993.tb06378.x
22. Zhang L, Peng H, Zhang W, Li Y, Liu L, Leng T. Yeast cell wall particle mediated nanotube-RNA delivery system loaded with miR365 antagomir for post-traumatic osteoarthritis therapy via oral route. *Theranostics*. 2020;10(19):8479–8493. doi:10.7150/thno.46761
23. Sabu C, Mufeedha P, Pramod K. Yeast-inspired drug delivery: biotechnology meets bioengineering and synthetic biology. *Expert Opin Drug Deliv*. 2019;16(1):27–41. doi:10.1080/17425247.2019.1551874
24. Yang F, Meng L, Lin S, Wu F, Liu J. Polyethyleneimine-complexed charge-reversed yeast cell walls for the enhanced oral delivery of pseudovirus-based antigens. *Chem Comm*. 2021;57(95):12768–12771. doi:10.1039/D1CC04901A
25. Kreger DR, Kopecká M. On the nature and formation of the fibrillar nets produced by protoplasts of Saccharomyces cerevisiae in liquid media: an electronmicroscopic, X-ray diffraction and chemical study. *J Gen Microbiol*. 1976;92(1):207–220. doi:10.1099/00221287-92-1-207
26. Rinaudo M. Non-covalent interactions in polysaccharide systems. *Macromol Biosci*. 2006;6(8):590–610. doi:10.1002/mabi.200600053
27. Xu X, Zhang X, Zhang L, Wu C. Collapse and association of denatured lentinan in water/dimethylsulfoxide solutions. *Biomacromolecules*. 2004;5(5):1893–1898. doi:10.1021/bm049785h
28. Zhang Y, Li S, Zhang L. Aggregation behavior of triple helical polysaccharide with low molecular weight in diluted aqueous solution. *J Phys Chem B*. 2010;114(15):4945–4954. doi:10.1021/jp9100398
29. Zhang R, Edgar KJ. Synthesis of curdlan derivatives regioselectively modified at C-6: o-(N)-Acylated 6-amino-6-deoxycurdlan. *Carbohydr Polym*. 2014;105:161–168. doi:10.1016/j.carbpol.2014.01.045
30. Meng Y, Lyu F, Xu X, Zhang L. Recent advances in chain conformation and bioactivities of triple-helix polysaccharides. *Biomacromolecules*. 2020;21(5):1653–1677. doi:10.1021/acs.biomac.9b01644
31. Duan B, Li M, Sun Y, Zou S, Xu X. Orally delivered antisense oligodeoxyribonucleotides of TNF-α via polysaccharide-based nanocomposites targeting intestinal inflammation. *Adv Healthcare Mater*. 2019;8(5):1801389. doi:10.1002/adhm.201801389